

Draft Manuscript – 1/14/2009 – Please do not cite or distribute without permission from the first author.

Possible explanations for the lack of trend in wet deposition of mercury at Underhill Vermont during a period of significant estimated mercury emissions reductions

Eric K. Miller, Richard Poirot, Jamie Shanley, Mark Cohen, Lynne Gratz, Miriam Pendelton, Sean Lawson, Melody Burkins, and Gerald Keeler

Abstract

The National Oceanic and Atmospheric Administration, US Environmental Protection Agency, Vermont Monitoring Cooperative, University of Vermont, Ecosystems Research Group, Ltd., University of Michigan, US Geological Survey, and Vermont Department of Environmental Conservation Air Quality Division have collaborated to measure atmospheric mercury deposition at Underhill VT (44.5283N, 72.8684W) on a storm-event basis since 1993. This 15-year event-based record provides unique insights into the climatology of mercury wet deposition in northern New England. There were major national (45%) and regional (54%) reductions of estimated mercury emissions during the period of observation. However, neither wet deposition nor the concentration of mercury in precipitation at Underhill declined in response to these reductions. Mercury deposition and concentration at Underhill were correlated with precipitation amount. Deposition was strongly seasonal and event driven with 44% of annual deposition occurring from June through August in conjunction with specific high-deposition events. Analysis of NOAA HYSPLIT model backward air mass trajectories indicated that likely source regions for high deposition events and the majority of annual deposition were located to the south and west in areas with high densities of coal-fired electric generating units (EGUs). In contrast to estimated total mercury emissions, estimated EGU emissions have been flat during the period of observation. Variation in precipitation amounts at Underhill and along transport paths appear to be responsible for much of the year-to-year variation in mercury wet deposition at Underhill, VT.

Introduction

Mercury is used in industry, medicine and dentistry, and in commercial products such as fluorescent lights, thermostats, switches, and thermometers. Mercury is also present as a trace contaminant in coal and oil. Mercury is released into the atmosphere when metal ores are smelted or coal, oil or municipal and medical wastes are combusted in facilities without proper pollution control technology. Large amounts of mercury have been released into the environment over the last several centuries by human activities, much of which is now stored in soils, vegetation, and lake sediments. Previously deposited anthropogenic mercury is re-emitted to the atmosphere by a process termed evasion and during forest fires.

Once deposited to the land or water a small fraction of mercury pollution is converted to the organic methyl-mercury form by bacteria active in anaerobic conditions. While it was recently thought that this methylation activity was restricted to throughoutly anoxic environments such as lake bottoms during summer stratification, recent research has shown the methylation process occurs widely in anerobic microsities in soils and sediments. Methyl-mercury is a potent neurotoxin and is readily concentrated in animal tissues. Methyl-mercury accumulates in both aquatic and terrestrial food webs (Rimmer et al. in preparation). Higher trophic level organisms with longer life-spans and slower growth rates exhibit the highest total and methyl-mercury burdens. Vermont and many other states have been forced to issue advisories against the consumption of popular fish species due their accumulated mercury levels. Emerging science is recognizing biologically significant mercury burdens in top-level consumer organisms in terrestrial food webs. There is particular concern about mercury impacts on insectivorous birds.

The atmospheric mercury observation program at Underhill, Vermont is designed to provide a comprehensive picture of atmospheric mercury pollution. The areas of investigation range from the temporal patterns of mercury concentration and speciation, to identification of sources of atmospheric mercury pollution arriving in Vermont, to direct measurements mercury deposition and evasion. The Underhill Air Quality Measurement site hosts a wide range of air pollution monitoring programs funded and operated by state and federal agencies. Other measurements include sulfur, nitrogen, and acid deposition, ground-level ozone, toxic substances, trace metals, fine particulate mass, UV-radiation, and meteorology. These additional measurements significantly enhance the ability to interpret the atmospheric mercury observations.

Atmospheric mercury research began at Underhill in 1992 when the University of Vermont and University of Michigan initiated a long-term monitoring program for mercury in precipitation. Precipitation samples are collected by an automated collector, which opens only during a precipitation event (Figure 1). In 2004 the Underhill Air Quality Site joined the NADP Mercury Deposition Network (MDN). Samplers using both the Michigan and MDN protocol were operated simultaneously for a period of 2 years after which event sampling was continued using only the MDN sampler and protocol. The record of mercury concentrations and deposition in individual rain and snow events at Underhill is the longest event-based record of mercury deposition in the world. During the 1990s pioneering studies of mercury accumulation in forest tree leaves, mercury in cloud water, and the wash-off of dry deposited material from tree leaves were conducted by UVM students in cooperation with UMAQL.



Figure 1. The University of Michigan MICB (left) and Mercury Deposition Network ACM (right) automated samplers for collecting mercury in precipitation. Moisture on a wetness-sensing element (on pole at upper right of the Michigan collector – not visible on the MDN collector) causes the lid to automatically open, exposing a clean sample train for collection of rainfall. Site operators exchange sample trains following each rain or snow event.

Several scientific papers have been published describing or using the information on atmospheric mercury collected at Underhill. Burke et al (1995) described the seasonal patterns in atmospheric mercury concentrations and deposition. Mercury concentrations and wet-deposition were highest in summer months and lowest in winter months, particularly when airflow associated with a precipitation event was from the south through west. Subsequent analyses using other wet deposition measurements throughout northeastern North America demonstrated that this seasonal pattern occurs throughout the region (Miller et al. 2005; VanArsdale et al. 2005).

In the late 1990s Lawson et al. (2003) and Malcom et al. (2003) investigated the concentration of mercury in cloud water near the summit of Mt. Mansfield adjacent to Underhill, Vermont. They found that mercury in cloud water was similar to but slightly higher (by a factor of 1.2) than the concentrations observed in precipitation. This difference can be explained by the generally smaller size (and lower water volume) of cloud droplets compared to rain droplets. Mercury does not appear to be as readily enriched in clouds droplets as are other pollutants such as sulfur and nitrogen. This is due to the exceedingly low concentrations of the soluble mercury forms (RGM and HGP) in the atmosphere and the very low water solubility of the dominant form

(GEM). Similar to the earlier results for precipitation (Burke et al. 1995), the highest cloud water concentrations were observed when airflow was from the southwest.

Keeler et al. (2005) described the record of mercury concentration and deposition in precipitation at Underhill measured by the Michigan MICB collector through 2003. Both Keeler et al. (2005) and VanArsdale et al. (2005) – who analyzed the Underhill data in conjunction with additional data from MDN sites in the region – determined that most of the annual mercury deposition in New England is associated with a small number of “high-deposition” periods or events, typically occurring from spring through early fall, when air-masses had traveled from the south and southwest to reach New England. These high deposition events appear to be associated with meteorological conditions that result in air-mass trajectories that bring air from high emissions density regions to the northeast during periods of vigorous convective mixing resulting in moderate to heavy rainfall (Keeler et al. 2005).

This paper analyzes the combined record from the Michigan MICB collector and NADP/MDN ACM collector through 2007. The additional years of observations increase the capability of the record for trend detection or rejection. New observations from the MDN collector from 2005 through 2007 are analyzed using air mass back trajectory methods to obtain further insights on factors controlling the timing and magnitude of mercury wet deposition in northern New England.

Methods

Study site

The Underhill, VT Air Quality Site (44.5283N, 72.8684W, 400-m elevation) is located in a rural setting on the campus of the University of Vermont Proctor Maple Research Center. Collectors are located in a clearing surrounded by northern hardwood forest. Situated on the western shoulder Mt. Mansfield, approximately 30 km east of Burlington, VT, the site is representative of deposition in the Lake Champlain Basin of Northern VT and NY. The site staff has extensive experience with precipitation collection through participation in NADP NTN, AIRMoN, MDN, VTDEC, and UMAQL networks. A site operator visits the site daily to facilitate event collection.

Precipitation collection and analysis using the MICB collector (1993-2006)

From 1993 to 2006 mercury wet deposition was monitored with the University of Michigan Air Quality Laboratory (UMAQL) protocol and UMAQL-modified MICB collector (Figure 1a, Burke et al. 1995, Keeler et al. 2006). Samples were analyzed at UMAQL following EPA method 1631.

Precipitation collection and analysis using the MDN ACM collector (2005-2007)

From 2005-2007 mercury wet deposition was monitored using the NADP Mercury Deposition Network (MDN) ACM (Figure 1b) sampler and protocol. Samples were analyzed following EPA Method 1631 at the MDN Hg Analytical Laboratory (HAL), Frontier Geosciences

in Seattle, WA. The sample protocol and sample processing are very similar to the UMAQL methods and are described in (Wetherbee et al. 2007).

Beginning in 2006 methyl mercury was analyzed in samples obtained with the MDN-ACM collector. Event-based analyses were conducted during the warm (June – October) season while monthly composite analyses were conducted during the remainder of the year. Methyl mercury was analyzed at the MDN HAL (<http://nadp.sws.uiuc.edu/lib/qaplans/HALqap2006.pdf>).

Blending data from two collection systems to create a long-term record

From 2005 to 2006 we operated both the MICB collection and analysis system and the MDN collection and analysis system on an event basis at Underhill (MDN site VT99). We conducted an exhaustive comparative performance analysis of the UMAQL-MICB, the MDN-ACM, and MDN-NCON collectors that is reported elsewhere (Miller et al. in preparation and Miller et al. 2008). From this study we developed transfer functions to relate concentration and deposition measured with each collector to measurements made with another. These transfer functions explained a high proportion of variance in the data ($r^2 = 0.9$) and are used to adjust for differential collection efficiencies of the two systems. We also determined that there was a stable and explainable bias between the MDN HAL and UMAQL laboratories on the basis of internal and external NIST-referenced QA samples provided by MDN and USGS (Greg Wetherbee, USGS personal communication 2008). The observed laboratory-laboratory bias of 9% was well within the performance requirements of EPA Method 1631 (77 -123%, USEPA 2002) to which both laboratories adhere. Still, this level of bias must be accounted for when comparing data from two different laboratories as we do here. To merge the time series, mercury concentrations from each laboratory were adjusted to a NIST recovery value of 100% based on the observed NIST recoveries. This adjustment eliminated the laboratory bias and eliminated the need to arbitrarily establish one laboratory or the other as the “best” measurement of concentration.

The two networks had different approaches to estimating precipitation amount with the UMAQL network using the precipitation catch of the collector (Landis and Keeler, 1997) and MDN using the precipitation measured by a co-located Belfort recording rain gage. Our comparative study demonstrated that the MICB precipitation collection was not significantly different from an NWS standard 8-inch gage, while the Belfort underestimated the NWS gage catch (Miller et al. in preparation). The long-term record was standardized to an NWS 8-inch precipitation gage basis. Deposition was calculated as the product of the NIST-referenced concentrations and NWS-gage referenced precipitation amounts.

Back trajectory analysis and source region identification

Air-mass backward trajectories for the 72 hours preceding air arrival at the receptor site were calculated using NOAA’s HYSPLIT model (Draxler et al. 2003) using EDAS 40-km resolution meteorology archived by NOAA. Trajectories were calculated in this study for a subset of all observations (2005-2007) corresponding to the MDN-network samples and because trajectory analysis for the period 1993-2003 had already been reported elsewhere (Keeler et al. 2005). A difficulty with calculating trajectories associated with precipitation events is associating air-mass arrival with precipitation collected. Earlier studies (e.g. Keeler et al. 2005) often selected a single “representative” trajectory associated with air arrival in the middle of or at the onset of the major precipitation associated with an event. From 2005-2007 we collected data from collector openings, tipping-bucket rain gage activity, relative humidity sensors, and a surface wetness sensor to document the periods of time when precipitation was occurring during the course (start to finish) of

an observed wet deposition event. We included in the analysis trajectories associated with all times of active precipitation during the 3-hour intervals. These trajectories were retrieved from a database of hourly trajectories developed for a companion study of ambient air mercury speciation (Miller et al. in preparation). Trajectory start heights for the primary trajectory data set were set to 500 m asl for the purposes of the ambient air speciation study. It is common practice to start trajectories at $\frac{1}{2}$ the mixed layer depth for precipitation studies (So.-Lai et al. 2007). The location of the Underhill site on the shoulder of Mt. Mansfield at 400 m asl places this site relatively high in the mixed layer – or at times above the mixed layer – and often at or just below cloud base during precipitation. Evaluation of mixed-layer depths during precipitation from the EDAS data indicated that the 500 m start height was appropriate for all 221 events analyzed in the trajectory study. Meteorological conditions (rainfall, air temperature, relative humidity, solar-flux, mixed layer depth) were extracted from the EDAS data for each trajectory endpoint time-location.

All hourly endpoints for trajectories originating at appropriate heights and times associated with each precipitation event were assigned the characteristics of each event at the receptor (concentration, precipitation amount, deposition). Trajectory endpoints with associated receptor conditions were aggregated into 1° degree latitude by 1° longitude grid cells. Descriptive statistics of receptor conditions associated with air passage over each grid cell were calculated. Maps were produced showing the number of times air arriving at the receptor during precipitation traversed each grid cell. Grid cells with fewer than 10 trajectory endpoints were removed from further analysis due to the limited representation of air traversing those locations at the receptor (Poirot and Wishinski, 1985). All GIS operations were conducted using IDRISI image processing software (Clark University <http://www.clarklabs.org>). These maps were used to identify likely source regions for high concentration and deposition events.

The potential source regions indicated by back-trajectory analysis were compared with a mercury emissions inventory (Cohen et al. 2004) to assess correspondence between potential source regions indicated by the trajectory analysis and known anthropogenic mercury emissions sources. The Cohen et al. (2004) inventory represents estimated emissions prior to the major regional reductions (~90%) in municipal waste combustor (MWC) and medical waste incinerator (MWI) emissions that occurred between 1998 and 2003. For this reason MWC and MWI emissions in the inventory were eliminated from this analysis of 2005-2007 precipitation events and trajectories. Because of uncertainty in trajectory endpoint locations due to numerical dispersion (Draxler et al. 2003) and the importance of large point sources to mercury emissions, the emissions data were aggregated into 1° latitude by 1° longitude grid cells for comparison with trajectory frequency. Specific precipitation events were associated with the emissions in a grid cell if any of the of the trajectory endpoints for an event fell within an emissions grid cell. Emissions were only associated with an event if the trajectory height in a given grid cell was below the mixed-layer height. If the trajectory height was above the mixed layer height at a grid cell, then it was assumed that the air mass transited that location without significant incorporation of emissions from within that cell as those emissions would likely be confined to the mixed layer. Emissions associated with specific event trajectories were also normalized for time-of-travel from source to receptor by dividing the emissions in a grid cell by the number of hours required to reach the receptor along the associated trajectory from that location. Time-of-travel normalized emissions were summed along all trajectories contributing to each event. Statistical analysis (described below) was conducted to explore the association of meteorological conditions and emissions along trajectories with deposition of mercury at the receptor.

Statistical analysis

Descriptive statistics, linear regressions, and ANOVA analyses were calculated using JMP 6.03 (SAS institute) statistical software. Data were natural log transformed as appropriate to obtain normal distributions prior to specific parametric analyses. Non-parametric Kendall family of trend tests were performed with the USGS computer program kendall.exe (Helsel et al. 2005 SIR 2005-5275 <http://pubs.usgs.gov/sir/2005/5275>). Seasonal Mann-Kendall p values were adjusted for serial correlation (Helsel et al. 2005) as there were more than 10 years of data available.

Results and Discussion

The NIST-referenced and collector efficiency-adjusted estimates of deposition for the two collector systems were comparable during the two years of overlap (2005:9.3/8.9, 2006:9.0/10.2 MICB/ACM). The difference between the two collector-protocol-laboratory systems (2005:-4.1%, 2006:+12%) was much less than the coefficient of variation for the time series (+/-20%) and within the expected range of agreement for two co-located MDN-ACM collectors as determined by Wetherbee et al. (2007). The adjusted MDN-ACM values obtained for 2005 and 2006 were used for this analysis.

Annual mercury wet deposition averaged 10.1 ug/m² from 1993-2007 with a precipitation-weighted mean concentration of 8.5 ng/L and average precipitation rate of 120 cm/year. There was considerable year-to-year variation in precipitation (Figure 2), mercury concentration (Figure 3), and mercury deposition (Figure 2). This variation was normally distributed (Shapiro-Wilk test) for precipitation amount and the precipitation-weighted mean concentration suggesting random processes influencing each. However, the distribution of annual mercury deposition was skewed slightly (median 9.21 ng/L, mean 10.1 ng/L).

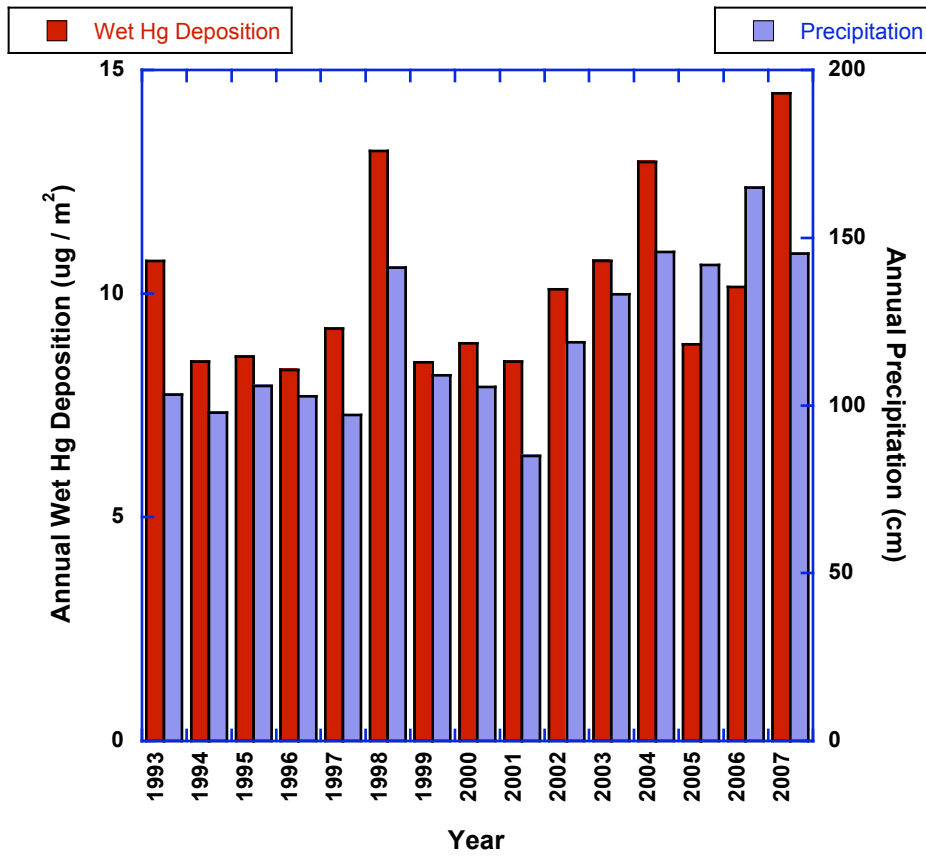


Figure 2. Annual precipitation and mercury wet deposition at Underhill, VT 1993-2007.

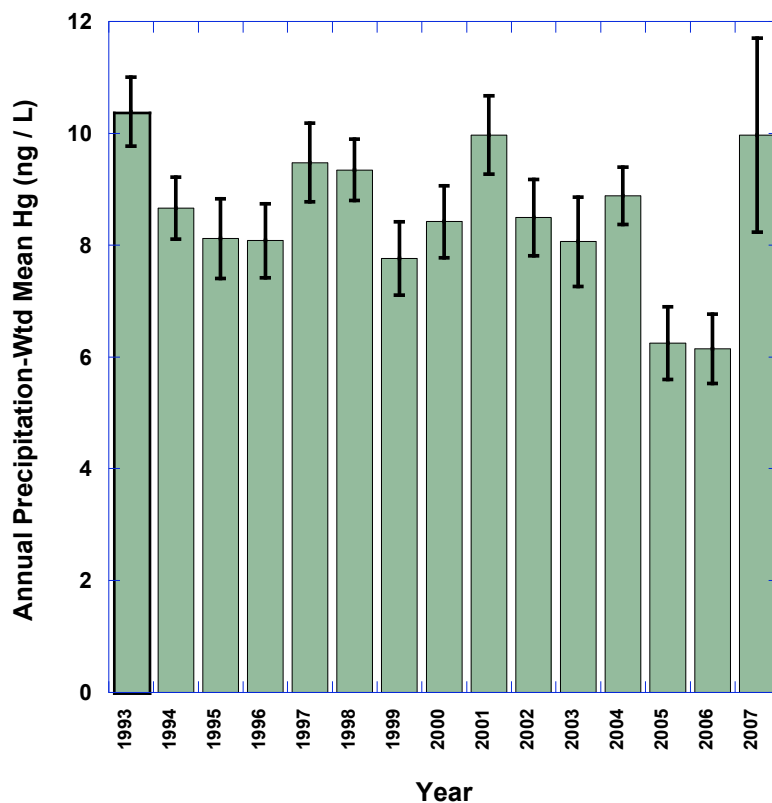


Figure 3. Annual precipitation-weighted mercury concentration in precipitation with standard errors.

Deposition was strongly seasonal with 44% of annual deposition occurring during summer (June-August) while only 10% of annual deposition occurred during winter (December-February) (Figure 4). Precipitation was also seasonal, but less so than mercury deposition (Figure 4). The proportions of precipitation delivered in summer and fall (September-November) precipitation were not significantly different at $p = 0.01$ (Tukey-Kramer HSD) with each season contributing just over 30% of annual precipitation. The proportion of annual precipitation delivered was significantly ($p = 0.01$) lower in winter (15%) and spring (March-May, 22%). Individual high-deposition events were responsible for a significant fraction of annual deposition. Two events (out of 1463) contributed more than 10% of annual deposition in their respective years, 22 events (1.5%) contributed more than 5% of annual deposition, and 498 events (34%) contributed more than 1% of annual deposition. High-deposition events were typically associated with air mass back trajectories to the south through west (Keeler et al. 2005, and discussed in detail below).

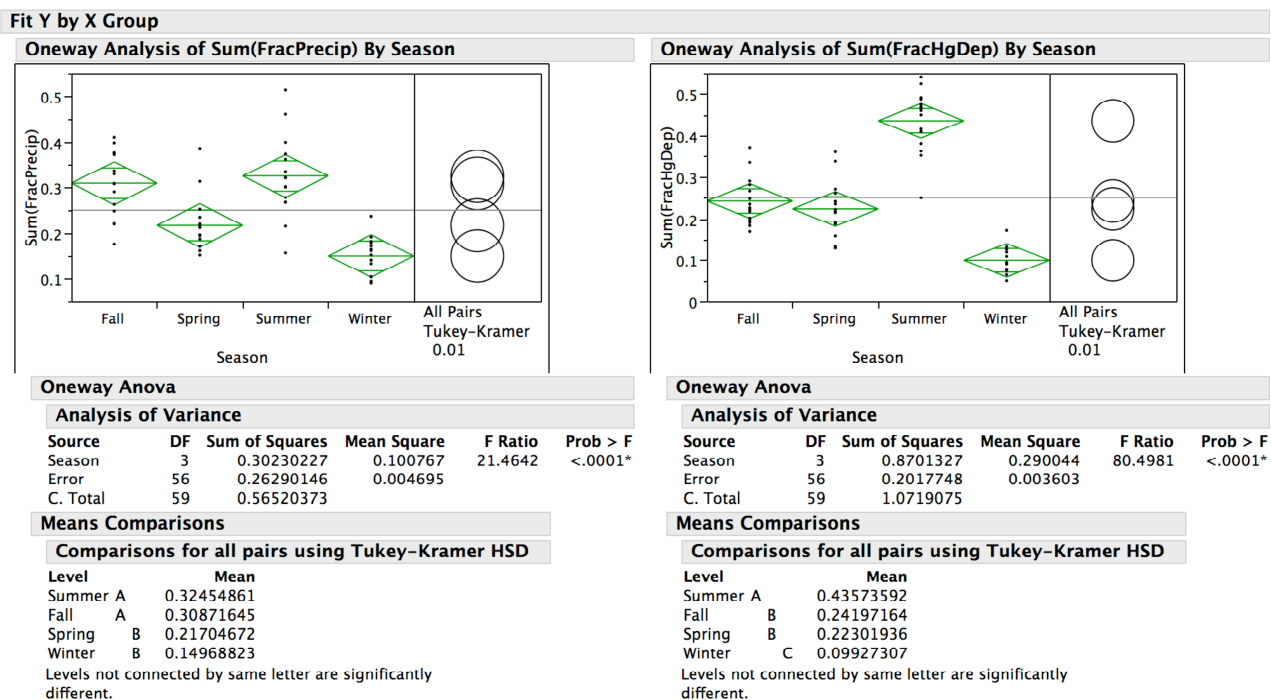


Figure 4. ANOVAs for the fraction of annual precipitation and fractional mercury wet deposition delivered by season (1993-2007).

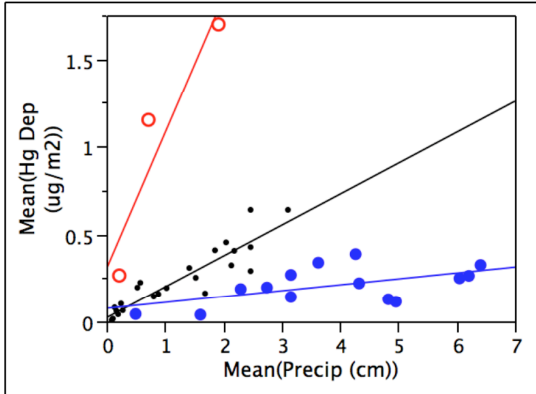
Potential mercury sources and meteorological influences on mercury deposition

There were consistent correlations between mercury wet deposition and precipitation amount by season suggesting stable sources and/or atmospheric production of divalent mercury available for scavenging in a given season. However, there were frequent outliers of either higher or lower apparent scavenging or higher or lower atmospheric Hg^{2+} levels in any given month (Figure 5, Table 1). The high and low outlier groups also showed consistent correlations with precipitation by season with either higher or lower slopes indicated (Figure 5, Table 1). The slopes of the regressions of wet deposition vs. precipitation were highest in summer and lowest in winter months (Figure 6, Table 1), consistent with the observed behavior of the volume weighted mean concentrations. The majority of events follow the intermediate deposition vs. precipitation trend group. We designate this trend (slope) the “normal” deposition dependence on precipitation rate. We designate the events falling on the higher slope trend for each season as the “high” deposition rate events, and the events falling on the lower slope trend for each season as the “low” deposition rate events.

11/18/08 5:32 PM

Data Table=June-July Subset of wet-traj-with-emiss-0d By
(WYear, WMonth, WDay, Season, Collection End Date)

Bivariate Fit of Mean(Hg Dep (ug/m2)) By Mean(Precip (cm))



— Linear Fit
— Linear Fit
— Linear Fit

Linear Fit

$$\text{Mean(Hg Dep (ug/m2))} = 0.0218845 + 0.1764932 \text{ Mean(Precip (cm))}$$

Summary of Fit

RSquare	0.827767
RSquare Adj	0.819938
Root Mean Square Error	0.078391
Mean of Response	0.235
Observations (or Sum Wgts)	24

Linear Fit

$$\text{Mean(Hg Dep (ug/m2))} = 0.3020808 + 0.7719432 \text{ Mean(Precip (cm))}$$

Summary of Fit

RSquare	0.869812
RSquare Adj	0.739625
Root Mean Square Error	0.369003
Mean of Response	1.038
Observations (or Sum Wgts)	3

Linear Fit

$$\text{Mean(Hg Dep (ug/m2))} = 0.0757006 + 0.0339338 \text{ Mean(Precip (cm))}$$

Summary of Fit

RSquare	0.3162
RSquare Adj	0.259217
Root Mean Square Error	0.091574
Mean of Response	0.207
Observations (or Sum Wgts)	14

Figure 5. Example separation of “high”, “normal”, and “low” deposition per unit precipitation trends. This example shows the combined events for June and July 2005-2007. The period 2005-2007 (the MDN record) is used here for consistency with the trajectory analysis presented below.

Table 1. Slopes, standard errors, and coefficients of determination for regressions of event wet mercury deposition ($\mu\text{g}/\text{m}^2$) against event precipitation (cm). The “normal” trend events were regressed by month. Due to the small number of observations of “high” and “low” trend events, these groups were regressed by two seasons (Fall-Winter-Spring and Summer). The values for the seasonal regressions are placed in the corresponding monthly positions in the table if there were events (data points) contributed to the seasonal regressions for a given month.

Month	HIGH Deposition			Normal Deposition			Low Deposition		
	Slope	SE	r ²	Slope	SE	r ²	Slope	SE	r ²
1	0.079	0.004	0.97	0.033	0.006	0.68	0.022	0.005	0.58
2	0.079	0.004	0.97	0.030	0.002	0.94	0.022	0.005	0.58
3	ne	ne	ne	0.131	0.013	0.91	0.022	0.005	0.58
4	ne	ne	ne	0.108	0.015	0.88	0.022	0.005	0.58
5	ne	ne	ne	0.118	0.023	0.66	0.022	0.005	0.58
6	ne	ne	ne	0.181	0.024	0.83	0.129	0.012	0.96
7	0.772	0.299	0.74	0.172	0.027	0.79	0.129	0.012	0.96
8	ne	ne	ne	0.098	0.009	0.86	0.129	0.012	0.96
9	ne	ne	ne	0.097	0.011	0.82	0.022	0.005	0.58
10	0.079	0.004	0.97	0.041	0.005	0.81	0.022	0.005	0.58
11	0.079	0.004	0.97	0.034	0.004	0.79	0.022	0.005	0.58
12	0.079	0.004	0.97	0.029	0.002	0.95	0.022	0.005	0.58

*ne - no high deposition events were detected during these months

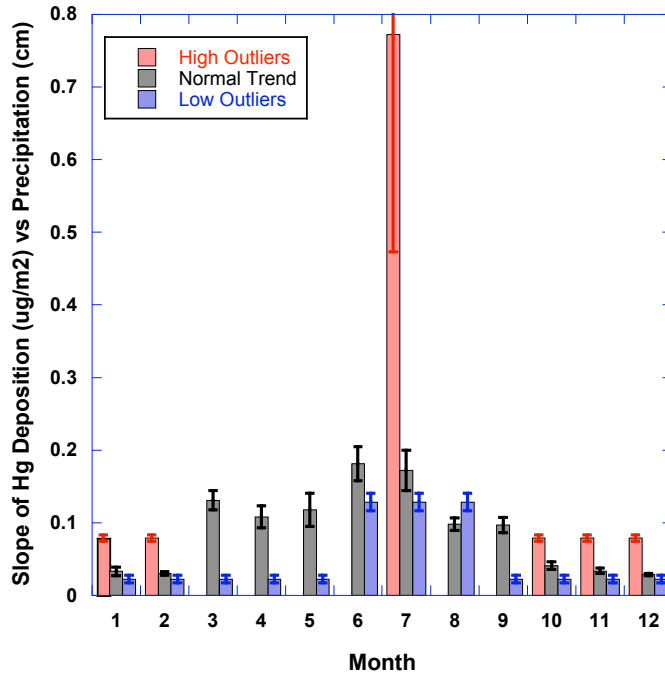


Figure 6. Slopes (with standard errors) of event wet mercury deposition ($\mu\text{g}/\text{m}^2$) against event precipitation (cm) by month (normal trend) and season (high and low trends).

Differences in emissions incorporated into the precipitating air-mass is a possible explanation for the different apparent functions of deposition with respect to precipitation amount (high, normal, low) in each season. Both total and time-of-travel normalized estimated mercury emissions along event back trajectories were higher for events in the group with higher deposition / precipitation slope than for the normal slope group when compared by season (ANOVA $p < 0.0001$, Figure 7). Both the total and normalized estimated emissions along the trajectories for the lower slope events were lower than those for the normal slope events, which in turn were lower than those for the high slope events ($p = 0.01$ means comparison, Figure 7). Back trajectories transited over lower estimated emissions regions during normal and low deposition events during summer than during other seasons (ANOVA $p = 0.01$, Figure 7). This was not true for high-deposition events for which the time-of-travel normalized estimated emissions along the back trajectories were not significantly different between seasons (t-test). These relationships suggest that different emissions levels associated with different transport pathways play a role in the increased or decreased deposition relative to precipitation amount relative to the normal trend in the high and low slope event groups (see additional discussion below).

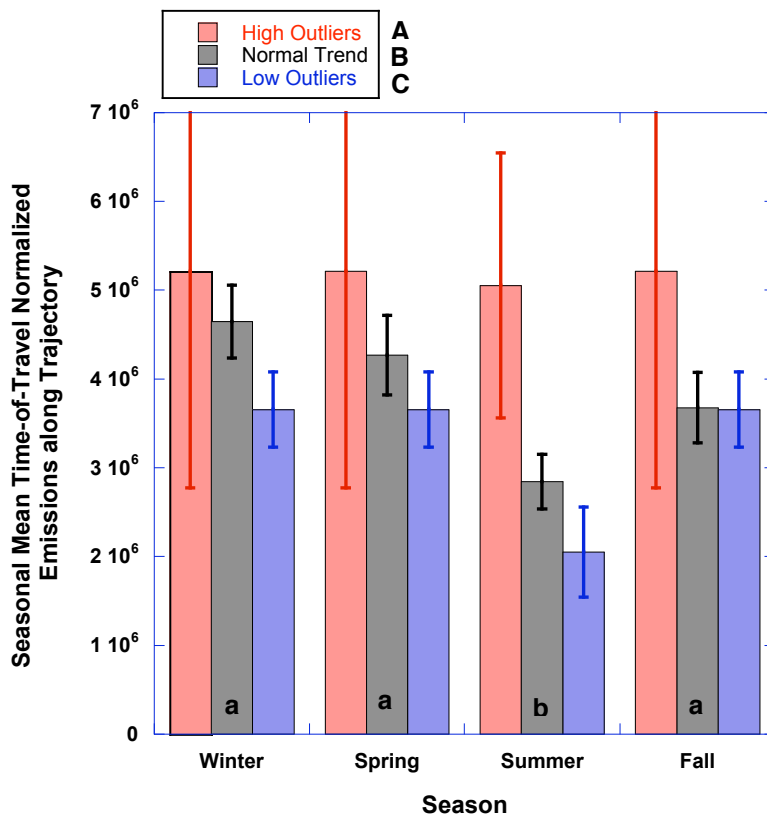


Figure 7. Time-of-travel normalized emissions along the back trajectories associated with precipitation events sampled at Underhill, VT during different seasons 2005-2007. Capital letters indicate significant ($p = 0.01$ means test) differences between event types (High, Normal, Low trends) across seasons using natural log transformed data (ANOVA $p < 0.0001$). Small letters indicate significant ($p = 0.01$ means test) between seasons for a given event type (ANOVA $p = 0.01$).

Low Hg deposition per unit precipitation events were associated with higher average precipitation amounts (mean 4.7 cm vs. 1.45 cm for high and normal trend events, $p=0.01$ means test, ANOVA $p<0.0001$). This relationship suggests a diluting effect of additional rainfall from low Hg trajectories providing a larger fraction of the precipitation than higher Hg trajectories during the event. Meteorological conditions along the back trajectory also differed by event type (high, normal, low slope). Low Hg deposition per unit precipitation events had higher humidity ($p=0.05$ means test, ANOVA $p=0.001$) and higher rainfall prior to arrival at the receptor ($p=0.05$ means test, ANOVA $p=0.029$). This suggests there was greater opportunity for scavenging and removal of atmospheric Hg^{2+} along the transport path prior to commencement of precipitation at Underhill. A general linear model including precipitation at the receptor, event type, trajectory mean solar flux, trajectory mean air temperature, and trajectory sum of emissions explained 83.7% of the variance in Hg wet deposition (Table 2). Thus, meteorological conditions and spatial variation in emissions along transport paths appear to regulate wet deposition rates at Underhill, VT. The substantial proportion of variance explained by the solar flux along the transport path is consistent with current models of photochemically driven oxidation of GEM to Hg^{2+} (Lin and Pekonnen 1999).

Table 2. General linear model results for mercury wet deposition as a function of precipitation amount at receptor site and meteorological conditions along air mass back trajectories for events sampled from 2005-2007. The bulk of the emissions signal is captured by the “Event Type” term (High, Normal, Low – see text).

2005-2007 221 Events Variance Explained Effect on Deposition p	PPT-R	TSunFlux	EventType	TSumEmiss	TAirT	Total
	55.9%	17.9%	8.6%	0.9%	0.5%	83.7%
	+	+	H+, L-	+	+	
	<0.0001	<0.0001	<0.0001	0.0003	0.0078	<0.0001

A challenge for identification of sources using event precipitation samples with back-trajectory analysis is that most precipitation event samples combine precipitation originating from different air masses arriving at different times over the many hours or days of a typical precipitation event. Therefore, multiple trajectories must be identified for each event and it is likely that only a few will describe the transport of the majority of the mercury contained in any given sample. The other trajectories will likely reflect additional precipitation from a non-source region that is diluting the sample.

A typical frontal-passage type rainfall scenario for Underhill involves low pressure to the north of the site and high pressure to the south both moving east. Initial flow is from the south and southwest sector, with flow shifting to the west and northwest as the front passes with precipitation occurring throughout the period. This general pattern is evident in Figure 8, which shows the frequency of trajectory hourly endpoints intersecting a grid cell for 221 precipitation events sampled at Underhill from 2005-2007. While there is clearly air arriving from eastern sectors associated with precipitation, the dominant pathways are from SSW, SW, W, and NW. Figure 8 also shows the total mercury emissions for each grid cell that was traversed by air arriving at Underhill in

association with precipitation. The largest emissions sources tend to occur in the south through west quadrant. There are no major mercury emission sources within 150 km of Underhill.

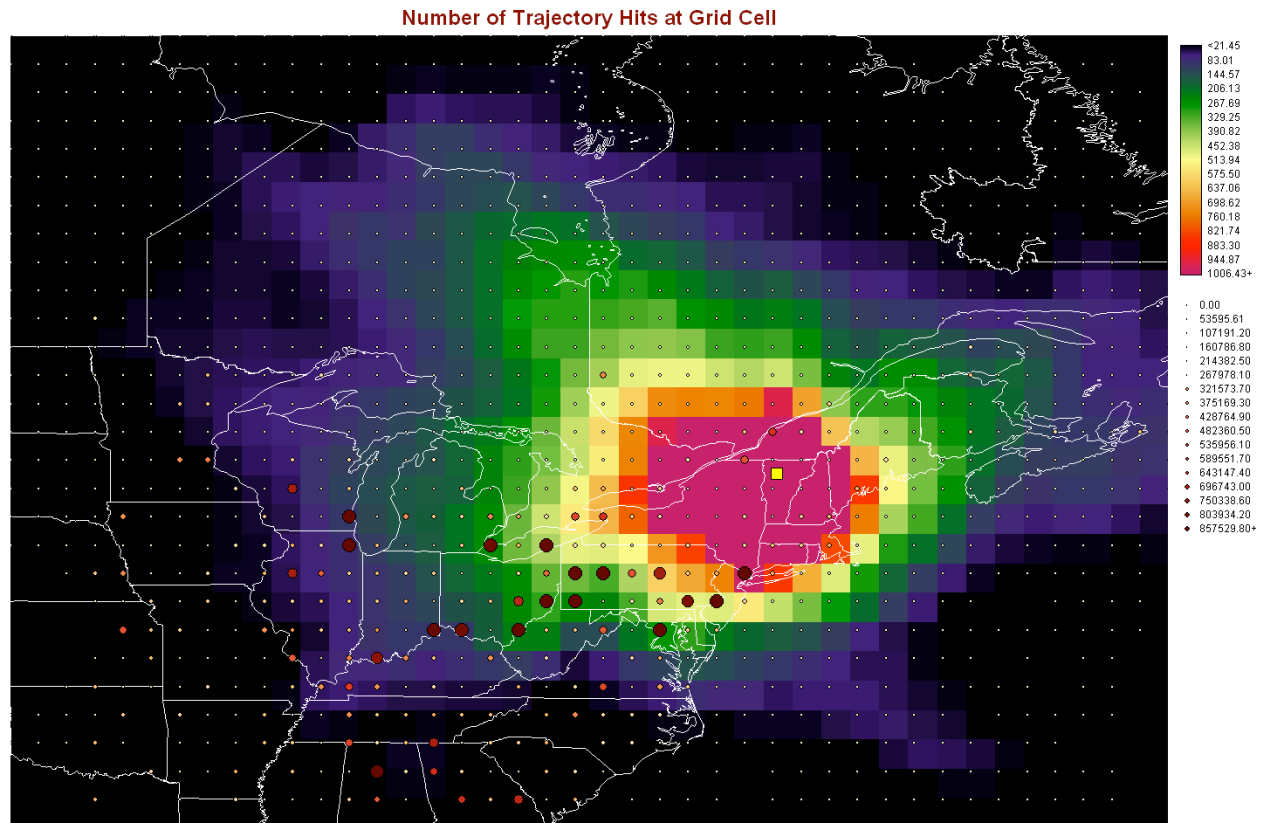


Figure 8. Mercury emissions sampled by air masses reaching Underhill, VT (large yellow square) during wet deposition events 2005-2007. The frequency of 72-hour trajectory endpoints falling in a grid cell is shown by the color shading of the grid cells, delineating the region of potential mercury sources. Overlaid on the grid are circles indicating (by color and size) the annual mercury emissions originating from each grid cell. The grid cells with both a high frequency of trajectory crossings and high mercury emissions are the most likely sources for the mercury in wet deposition at Underhill, Vt.

Figure 9 shows the frequency of air masses transiting grid cells for only the “high” deposition regime events. The SW and NW corridors are dominant transport paths for these types of events. As an example, all of the trajectories associated with precipitation occurring during the event collected on 7/17/2005 are presented in figure 9. This event provided the highest fraction of annual deposition of any event in the full time series (11.7%). It seems likely that the bulk of the mercury in this event was contributed by the major sources in NJ, central and western PA, OH, and possibly from the very large but distant source region near Chicago IL. None of the trajectories associated with this event crossed the much smaller magnitude, but more proximal sources in QC. Similar patterns are evident for the other high deposition events with the W through NW corridor reflecting air arriving during the end of the precipitation events.

There was a significant difference in the location of trajectory endpoints by event type (Table 3). High deposition per unit precipitation events had 47.1% of their trajectory endpoints in

the SW quadrant relative to the receptor, while low deposition events had only 20.4% in the SW sector. Conversely, Low deposition events had 28.8% of trajectory endpoints in the eastern sectors, while high deposition events had only 15.5% in the eastern sectors. All three event types had ~35% of trajectory endpoints in the NW sector. The spatial-mean annual estimated Hg emissions sampled by trajectory endpoints were significantly different by quadrant. Spatial-mean annual estimated emissions sampled by trajectory endpoints in the SW sector were 3 times greater than those from any other quadrant. Thus the high-deposition regime can be characterized as atmospheric circulation conditions that favor precipitation during south to west flow from the high emissions sector with less precipitation contributed to each event in association with flow from much lower emissions sectors to the east. The low deposition regime can be characterized as atmospheric circulation conditions that favor precipitation occurring during flow from the low emissions eastern region with less precipitation contributed in association with flow from the high-emission region (SW).

Table 3. Summary of trajectory endpoint frequency by event type and quadrant relative to receptor location and summary of spatial-mean annual Hg emissions sampled by trajectory endpoints by quadrant relative to receptor. Trajectory endpoint frequency was significantly different by quadrant ($p < 0.00005$). Mean annual estimated emissions were significantly different by quadrant (ANOVA $p < 0.00005$) with each quadrant's estimated emissions significantly different from all others (Tukey-Kramer HSD means test $p = 0.01$).

Trajectory Quadrant	NE	NW	SE	SW
Event Type				
High Dep/PPT	9.1%	37.4%	6.4%	47.1%
Normal Dep/PTT	13.3%	37.5%	15.5%	33.8%
Low Dep/PPT	27.7%	32.9%	19.1%	20.4%
Mean Estimated Emissions (g/y)	41,646	62,026	71,561	211,656

The attribution of significant wet deposition of mercury at Underhill to the EGU and industrial sources in the S through W quadrant is consistent with the potential source contribution analysis conducted by Miller et al. (in preparation) for ambient vapor-phase mercury measured at Underhill. In the ambient air study, a single trajectory can be associated with each 2-hour integrated sample, thus making plain the dominance of the known sources in the S through W quadrant. S.-o Lai et al. (2007) also identified qualitatively similar source regions contributing to wet deposition of mercury sampled at Pottsdam, NY (44°40'N, 74°59'W, ~170 km almost due west of Underhill) during 2004 and 2005.

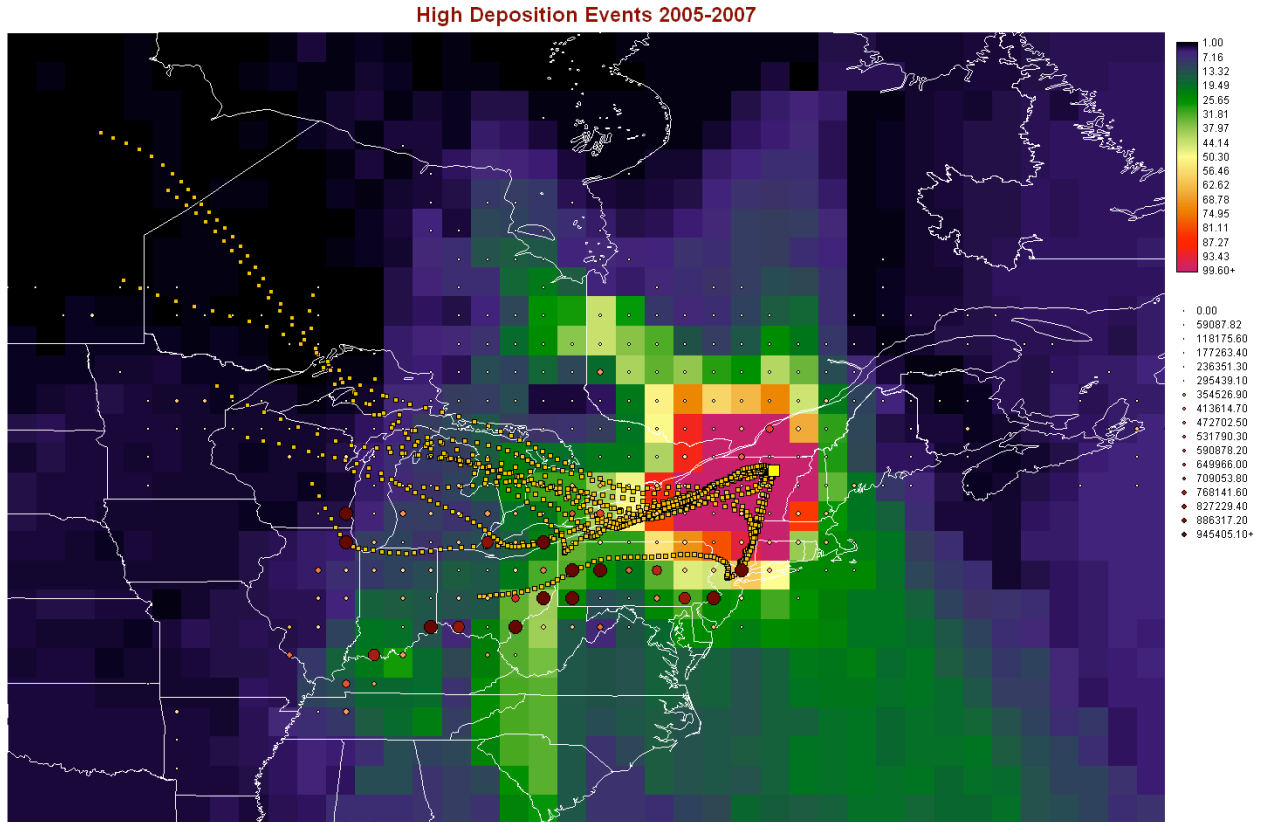


Figure 9. Mercury emissions sampled by air masses reaching Underhill, VT (large yellow square) during “High” deposition type precipitation events 2005-2007 (see text). The frequency of trajectory endpoints falling in a grid cell is shown by the color shading of the grid cells, illustrating the region of potential mercury sources. Overlaid on the grid are circles indicating (by color and size) the annual emissions from each grid cell (g/y). The grid cells with both a high frequency of trajectory crossing and high mercury emissions are the most likely sources for the mercury in wet deposition at Underhill, Vt. Overlaid in small yellow squares are the hourly (72-hours) HYSPLIT backward trajectory endpoints associated with precipitating periods during the event with collection ending on 7/17/2007. This single event provided the highest fraction of annual deposition of any event collected in the 15-year record. Major mercury emissions sources in NJ, central and western PA, OH, and possibly even IL contributed to this extreme event.

No trend in precipitation mercury despite significant estimated emissions reductions

The mercury wet deposition record at Underhill, VT (1993 – 2007) covered an important period when estimated US mercury emissions fell by 45% (1990 – 1999; USEPA, www.epa.gov) and estimated emissions in the Northeastern states and Eastern Canadian Provinces dropped by 54% during 1998-2003 (C. Mark Smith, NESCAUM 2004 Mercury Conference, Portland ME). Despite the apparently significant mercury emissions reductions achieved during the period of observation, there were no significant declining trends in mercury wet deposition or concentration detected by either annual or seasonal Mann-Kendall tests (Figure 2). This is likely due to the apparent significant influence of long-range transport of EGU mercury emissions on a large portion of the annual mercury deposition at Underhill. Estimated EGU emissions were constant both nationally and regionally during the period of observation (USEPA, C. Mark Smith, NESCAUM 2004 Mercury Conference, Portland ME). The apparent emissions reductions were achieved through controls on medical waste incinerators and municipal waste combustors along with the closing of a chlor-alkali plant in Maine.

Alternatively, it is also possible that emissions reductions were overestimated for the period. Also, remission from soils of previously deposited anthropogenic Hg that would be concentrated near large sources could compensate for some of the estimated recent emissions reductions. Others have suggested that increases in emissions sources such as fires in northern peatlands (<http://www.usgs.gov/newsroom/article.asp?ID=1550>) may offset recent estimated emissions reductions. However, the trajectory analysis presented above does not indicate any strong influence from the region of these northern peatlands.

As would be expected from their high correlation on an event basis, annual mercury wet deposition increased linearly with annual precipitation, while concentration decreased linearly with annual precipitation (4 outlier years excluded, Figure 10). The 4 outlier years (1993, 1998, 2004, and 2007) with annual precipitation-weighted mean mercury concentrations above the long-term average dilution line (Figure 4) were also the 4 highest deposition years. These four years had a greater proportion of “high-deposition” type events where the Hg concentration was high relative the precipitation amount (14-19 events as compared to an average of 11 events for the on-trend years). High-deposition events were responsible for 45 to 63% of annual deposition in the outlier years as opposed to 32% of annual deposition for on-trend years. The high deposition years were distributed throughout the record.

Butler et al. (2007) studied the much shorter record (1998-2005) available for NADP/MDN sites and identified a declining trend in precipitation concentration with no trend in wet deposition for the eastern US sites during this shorter period. They attributed this short-term decline in precipitation mercury concentration to declines in anthropogenic mercury emissions nationally and regionally. The much longer record of observation at Underhill indicates that the 1998-2005 decline in precipitation mercury concentration was a short-term cycle within a long-term period with no trend (Figures 2,3). Our analysis suggests that the most plausible explanation for this string of nominally declining concentration years is largely the result of increasing precipitation during the period. The period of 1998-2005 can be seen as typical of the range of variation present over 15 years with no long-period trends (Figures 2,3). Furthermore, the bulk of estimated anthropogenic emissions reductions were accomplished between 1990 and 1999 before the MDN observation

record began. There was no clear signal of these major reductions in the 1993-2007 record at Underhill.

Variations in climate (precipitation amount and atmospheric circulation – frequency of storms in air with favored trajectories) explain much of the year-to-year variation in mercury deposition at Underhill, VT. The high contribution of “high-deposition” events resulting from air masses traversing the high emissions regions to the south and west with multiple EGUs to the annual deposition likely explains the lack of any temporal signal associated with large national and regional estimated mercury emissions reductions from municipal waste combustors and medical waste incinerators during the period of observation.

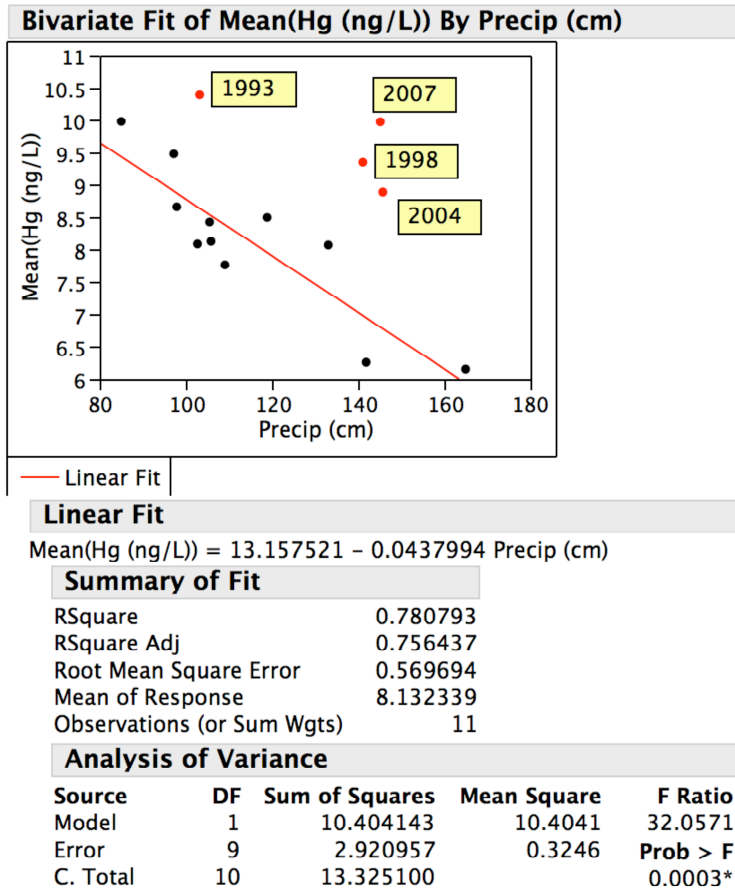
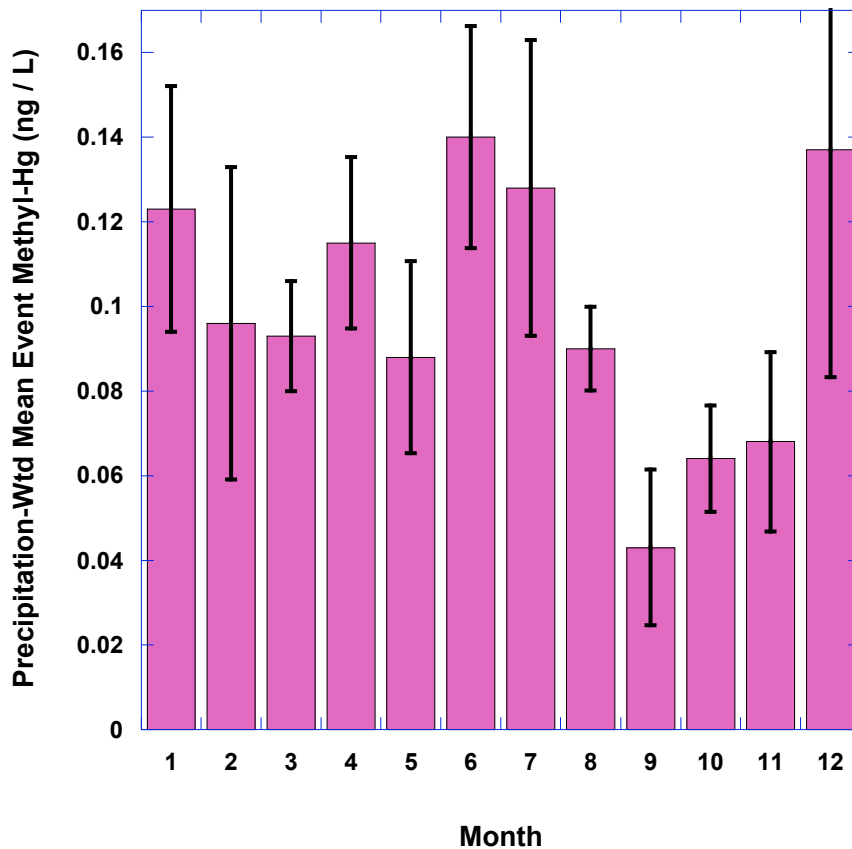


Figure 10. Precipitation “dilution effect” on mean annual mercury concentration in precipitation. The four outlier years (removed from regression) had unusually high mercury concentrations relative to precipitation amounts for the period resulting in the 4 highest deposition years of the record.

Methyl Mercury

As has been observed elsewhere, trace amounts of methyl mercury (range 0.07-3.93%, mean 1.2% of total mercury) are present in precipitation sampled at Underhill, VT (Figure 11). The source of methyl mercury in precipitation is not clearly established and may be varied, but the

majority seems quite likely to be the result of aqueous phase methylation of non-particle bound Hg^{2+} (Hammerschmidt et al. 2007). With the exclusion of two outliers (the top 2 high deposition events for total mercury 11.7% and 7.9% of annual deposition during the methyl mercury sampling period 2005-2007), methyl mercury concentration was positively linearly correlated with total mercury concentration ($r^2 = 0.40$, $p = 0.0005$). This correlation is consistent with Hammerschmidt et al.'s (2007) hypothesis. A provisional estimate of the annual deposition of methyl mercury is $76.5 - 162 \text{ ng/m}^2/\text{y}$ (central estimate $116 \text{ ng/m}^2/\text{y}$) derived by multiplying the monthly volume-weighted mean methyl mercury concentrations (Figure 11) by the average monthly precipitation and propagating uncertainties. This flux represents a significant delivery of methyl mercury to terrestrial and aquatic ecosystems in the region.



Acknowledgements

The atmospheric mercury observation program at Underhill, Vermont would not be possible without the dedicated efforts of VMC staff members Mim Pendleton, Carl Waite, and Judy Rosvosky. These individuals maintain and operate the monitoring equipment and their hard work in all kinds of weather has been responsible for the high quality of the extensive observational record. The authors gratefully acknowledge the NOAA Air Resources Laboratory (ARL) for the provision of the HYSPLIT transport and dispersion model used in this publication. Funding for this research was provided by NOAA, EPA, VTANR, and USGS.

References

- Burke, J., M. Hoyer, G. Keeler, and T. Scherbatskoy. 1995. Wet deposition of mercury and ambient mercury concentrations at a site in the Lake Champlain Basin. *Water Air and Soil Pollution* 80:353-362.
- Butler, T.J., M.D. Cohen, F.M. Vermeulen, G.E. Likens, D. Schmeltz, and R.S. Artz. (2008) Regional precipitation mercury trends in the eastern USA, 1998-2005: Declines in the Northeast and Midwest, no trend in the Southeast. *Atmos. Environ.* DOI:10.1016/j.atmosenv.2007.10.084.
- Cohen, M., R. Artz, R. Draxler, P. Miller, D. Niemi, D., D. Ratte, M. Deslauriers, R. Duvar, R., Laurin, J. Slotnick, T. Nettesheim, and J. McDonald. (2004) Modeling the atmospheric transport and deposition of mercury to the Great Lakes. *Environmental Research* 95:, 247-265.
- Draxler, R.R. and Rolph, G.D., 2003. HYSPLIT (HYbrid Single-Particle Lagrangian Integrated Trajectory) Model access via NOAA ARL READY Website (<http://gus.arlhq.noaa.gov/ready/open/hysplit4.html>). NOAA Air Resources Laboratory, Silver Spring, MD.
- Hammerschmidt, C. R., C.H. Lamborg, and W.F. Fitzgerald. (2007) Aqueous phase methylation as a potential source of methylmercury in wet deposition. *Atmos. Environ.* 41:1663-1668.
- Keeler, G.J., L.E.Gratz, and K. Al-Wali. (2005) Long-term Atmospheric Mercury Wet Deposition at Underhill, Vermont. *Ecotoxicology* 14, 71 –83.
- Lawson, S.T., Cloud water and throughfall deposition of mercury and trace elements in a high-elevation spruce-fir forest at Mt. Mansfield, Vermont. (2003) *Journal of Environmental Monitoring* 5, 578-583.
- Malcom, E.G., G.J. Keeler, S.T. Lawson, and T. Scherbatskoy. (2003) Mercury and trace elements in cloud water and precipitation collected on Mt. Mansfield, Vermont. *Journal of Environmental Monitoring* 5, 584-590.
- Miller, E.K., VanArsdale, A., Keeler, G.J., Chalmers, A., Poissant, L., Kamman, N., and Brulotte, R. (2005) Estimation and Mapping of Wet and Dry Mercury Deposition across Northeastern North America. *Ecotoxicology* 14, 53-70.
- Poirot, R.L. and P.R. Wishinski (1985). Regional apportionment of ambient sulfate contributions to a remote site in northern VT. *Transactions APCA Int. Spec. Conf. on Receptor Modeling: Real World Issues and Applications*, T.G. Pace, Ed., pp. 239-250, Williamsburg, VA.
- Rimmer, C.C., McFarland, K.P., Evers, D.C., Miller, E.K., Aubry, Y., Busby, D., and Taylor, R.J. (2005) Mercury Levels in Bicknell's Thrush and Other Insectivorous Passerines in Montane Forests of Northeastern North America. *Ecotoxicology* 14, 223-240.
- Lai, S.-o , T. M. Holsen, P. K. Hopke, and P. Liu. (2007) Wet deposition of mercury at a New York state rural site: Concentrations, fluxes, and source areas. *Atmos. Environ.* 41:4337-4348.
- USEPA (2002) Method 1631, Revision E: Mercury in Water by Oxidation, Purge and Trap, and Cold-Vapor Atomic Fluorescence Spectrometry. www.epa.gov
- VanArsdale, A., Weiss, J., Keeler, G.J., Miller, E.K., Boulet, G., Brulotte, R., Poissant, L., and Puckett, K. (2005) Patterns of Mercury Deposition in Northeastern North America (1996-2002). *Ecotoxicology* 14, 37-52.

Wetherbee, G.A., D. A. Gay, R.C. Brunette, and C.W. Sweet. (2007) Estimated variability of National Atmospheric Deposition Program/Mercury Deposition Network Measurements using collocated samplers. *Environ. Mon. Assess.* DOI 10.1007/s10661-006-9456-6.